

Mechatronic face mask anti covid-19 to remotely record cardiorespiratory variables in farm's workers engaged in jobs at high risk of infection

Original

Mechatronic face mask anti covid-19 to remotely record cardiorespiratory variables in farm's workers engaged in jobs at high risk of infection / Velluzzi, F.; Fois, A.; Dell'Osa, A. H.; Tocco, F.; Manuello Bertetto, A.; Serra, C.; Melis, L.; Bertelli, U.; Concu, A.. - In: INTERNATIONAL JOURNAL OF MECHANICS AND CONTROL. - ISSN 1590-8844. - 22:1(2021), pp. 61-76.

Availability:

This version is available at: 11583/2961164 since: 2022-04-13T10:03:16Z

Publisher:

Levrotto and Bella

Published

DOI:

Terms of use:

openAccess

This article is made available under terms and conditions as specified in the corresponding bibliographic description in the repository

Publisher copyright

(Article begins on next page)

MECHATRONIC FACE MASK ANTI COVID-19 TO REMOTELY RECORD CARDIORESPIRATORY VARIABLES IN FARM'S WORKERS ENGAGED IN JOBS AT HIGH RISK OF INFECTION

Fernanda Velluzzi¹, Andrea Fois², Antonio Hector Dell'Osa³, Filippo Tocco⁴, Andrea Manuello Bertetto⁵
Carmen Serra⁵, Laura Melis⁶, Ugo Bertelli⁷, Alberto Concu⁸

¹ Obesity Centre, Department of Medical Sciences and Public Health, University of Cagliari, Italy;

² Remote Biosignal Acquisition Unit, Nomadyca Ltd, Kampala, Uganda;

³ Instituto de Desarrollo Economico e Innovacion, Universidad Nacional de Tierra del Fuego, Ushuaia, Argentina;

⁴ Sports Medicine Lab, Department of Medical Sciences and Public Health, University of Cagliari, Italy;

⁵ Department of Mechanics and Aerospace Engineering, Politecnico di Torino, Italy;

⁶ Medical Faculty at the Bucarest Universitatea din Medicina si Farmacie Carol Davila, Bucarest, Romania;

⁷ Blue Matrix Ltd, Taranto, Italy;

⁸ 2C Technologies Ltd, Accademic SpinOff at the University of Cagliari, Italy.

ABSTRACT

The most frequent prodromes of COVID-19 infection are fever, signs of respiratory diseases, cough and shortness of breath. Nevertheless, it is not infrequent that patients with COVID-19 also show cardiac symptoms. So, it is of importance to detect the prodromal symptoms of the COVID-19 infection in order to be able to make a diagnosis as quickly as possible to provide the immediate insertion of the infected people in isolation/therapy protocols. Here is presented a prototype of a smart face mask, named AG47-SmartMask that, in addition to the function of both an active and passive anti COVID-19 filter by an electro-heated filter brought to a minimum temperature of 38°C, it also allows the continuous monitoring of numerous cardio-pulmonary variables. Several specific sensors are incorporated into the mask to assess the inside mask temperature from which synchronous waving with the breathing was acquired the breath frequency, relative humidity, air pressure together and end tidal carbon dioxide percentage, and an auricular assessment of the body temperature, the heart rate and the percentage of oxygen saturation of haemoglobin. Sensors are embedded within an advanced ICT platform. To validate the AG47-SmartMask tool, were engaged twenty seven Farm's workers of a vegetable packaging chain and they dressed the face mask device to simulate, while working, both tachypnea and cough, and the AG47-SmartMask faithfully quantified the simulated dyspnoic events.

Keywords: COVID-19, smart face mask, electro-heating active filtering, wearable biophysical sensors, telemedicine platform.

1 INTRODUCTION

The latest scientific and clinical evidence makes it clear that the covid-19 pandemic, which started just over 2 years ago, still shows no signs of significantly reducing its virulence or lethality in the world [1].

The reasons for all this happening are rather complex both on the purely health level and on the broader socio-cultural and economic level. Certainly, the rapid spread of vaccines against covid-19 that is occurring all over the world promises to mitigate the risk of exponential growth of infections [2]. However, it cannot be ruled out that this risk may persist for an even longer time, especially in those geographic areas of the planet with the highest population density accompanied by a chronic low efficiency of national health systems [3].

Contact author: Alberto Concu

2C Technologies Ltd, Via Ravenna 24, 09 125 Cagliari, Italy.
E-mail: aconcu44@gmail.com.

Now paying attention more focussed to the environments of those workers who, for reasons deriving from the type of job, may be particularly exposed to COVID-19 infection, that of farm workers seems to be particularly vulnerable [4]. In fact, it has been found that in the context of agricultural workers, COVID-19 overlaps with the disparate health problems that they often suffer as they are long lasting exposed to environmental risks such as pesticides, excessive temperature changes, and who suffer from occupational diseases such as arthritis and others muscle disorders as well as often they suffer from severe kidney disorders [5]. During the COVID-19 pandemic, work environments poorly protected from infection, typical of the farm's working and living condition, expose these workers to a greater risk of corona virus infection. For example, many harvesters have to work side by side, share transportation and housing, migrate between farms, and may have inadequate access to facilities where they can wash their hands and clothing. For these reasons, the canonical rules for the individual protection from infection must continue to be observed for an extended time, the duration of which is not foreseeable at the moment. Among the individual protection systems from COVID-19 infection, the one that remains the simplest but also the safest is represented by the maintenance of the optimal inter-individual distance accompanied by the wearing of appropriate devices/barriers which, at the level of the environment air access in the respiratory system, or rather of the mouth and nose, greatly reduce, if not even cancel, the access of risky viral loads: we are therefore talking about facial masks[6]! However, the use of disposable face masks is creating a huge global problem for the disposal, in an environmentally sustainable way, of these health facilities [7].

Putting these problems together, it is mandatory to have personal protective equipment from COVID-19 as soon as possible, in the form of face masks, which implement the two characteristics of high virus filtering capacity and be usable for long periods of time thanks to appropriate intrinsic systems of periodic sanitation, thus eliminating the problem of the accumulation of these disposable products in the environment. Another feature that these devices for facial protection from COVID-19 infection would have, beside being tools with therapeutic value, that is, the blocking of infectious agents towards the airways, should be of providing information, in real time, concerning the possible prodromes of infection through a system of specific micro sensors embedded in the facial mask tissue that are able to send such information towards a remote control medical stations. The creation of facial devices with similar characteristics could also be of not negligible importance, especially for health care and civil protection workers who are most exposed to the infection, since these tools could detect the prodromal symptoms of this infection in order to be able to make a diagnosis of possible positivity to COVID-19 infection as quickly as possible and therefore to provide their immediate insertion in the isolation/therapy protocols.

However, the risk of contracting the COVID-19 infection also occurs for workers in other production areas such as the agriculture workers, the workers on industrial production lines with mobile workstations that involve workers frequently approaching each other, and employees working in service companies whose workstations are closely spaced and located in open work spaces, the military operating in action groups that involve close individual proximity. Even people who practice sports in closed environments, being particularly at risk of contracting the COVID-19 infection, can increase their level of safety from this infection thanks to the use of these instrumented facial devices. In a paper accepted for the presentation at the 2021 IEEE/MeMeA Symposium on Medical Measurements and Applications [8], we have proposed a preliminary prototype of a non-disposable face mask instrumented by a mini sensor inside it, suitable for detecting the variations, breath-by-breath, of the temperature, the percentage of humidity and the pressure, which are established inside the mask and which allow, with good approximation, to have above all information on the respiratory rate trend since, as is known, alterations in the respiratory rhythm can be early symptoms of the incipient implementation of the COVID-19 infection. Starting from this encouraging first result, with this work we have further improved the first prototype of face-mask, called AG-47 SmartMask, for the purpose of having it an important leap of performance, especially as regards the quality of the materials used for its construction and its self-filtering system, the quality and quantity of sensors embedded within it and the proprietary software suitable for the remote acquisition, normalization, transmission and, particularly, for refine a lot the controls of the numerous biophysical signals so acquired that, taken together, they can effectively contribute to giving early signals of risk of loss of capacity of homeostasis of the most important systems of the organism as these are preferred targets of COVID-19.

2 METHODS

2.1 FACE MASK

The APVR AG-47 SmartMask device consists of an intelligent respiratory protection device, equipped with a large number of sensors and sophisticated control electronics. Thanks to the presence of numerous sensors capable of continuously and non-invasively sampling a large number of physical and chemical parameters relating to the internal and external environment of the face mask, the AG-47 SmartMask therefore represents a sensitive and precise sampling tool fast and low cost. The sensors of the device are able to measure tens of times per second (i.e. with frequencies between ~ 10 Hz and 10^2 Hz) the parameters of interest without the need for any action by the user, making it possible to reconstruct even the smallest variations in the observed parameters. The complete integration of the sensors inside the face mask also makes the deployment and use of the device extremely simple and

rapid in multiple use scenarios which can vary, by way of example, from industrial work environments to domestic ones up to healthcare ones. The use of the device by the end user who wears it appears to be, in the basic mode, identical to the use of a common APVR device (such as a common surgical face mask). However, the device is able to offer, even to the end user, a series of advanced features designed to better support work-related activities and facilitate the continuous use of face masks during their performance. The signals sampled in continuous mode from the sensor set of the AG-47 SmartMask are acquired and recorded in real time by the electronic control system of the device. These signals are recorded in a protected way inside the storage area of the AG-47 SmartMask and can be transmitted, through connections protected by strong encryption, to a mobile device (e.g. smartphone or tablet PC) connected to the mask. The acquired signals are translated by the electronic control system of the AG-47 SmartMask respirator into biosignal traces that are filtered and analyzed in real time, in order to obtain an extraction of the features of interest present in them. The analysis and filtering work synergistically on the acquired data thanks to the use of data fusion models and highly optimized and pre-trained artificial intelligence systems for the specific analysis of the signals considered. The original signals and the set of obtained features points are transmitted directly or indirectly (through a mobile application that was specifically developed for these purposes as part of the project) to the system's telemedicine platform, the AG-47 RTP (Remote Telemedicine Platform). The AG-47 RTP, by carrying out an advanced analysis of the temporal dynamics presented by the signals and by the relative feature points extracted from them, is able, by making intensive use of machine learning techniques, to detect early the most frequent prodrome of COVID-19 infection, from the earliest stages of infection. Thanks to this continuous monitoring, the diagnostic functions, and the early detection of prodromal symptoms of the pathogen, the AG-47 platform allows as a whole to obtain a very rapid isolation of potentially infected subjects and a timely health intervention on them, to avoid evolutions. of morbidity.

2.1.2 External shell

The external structure of the AG-47 SmartMask consists of a plastic material casing that has been designed to ensure maximum adherence to the user's face, creating an almost sealed breathing chamber. The design and the internal and external volumes of the respirator's facial envelope were also designed to house the functional components of the SmartMask (sensors, filters, electrical connections, etc.) and the prototypes used were obtained by means of 3D printing, as shown in the figure 1 shown below.

In the upper part of the Figure 1 it's possible to see the three-dimensional models of the external envelope of the AG-47 SmartMask in the pre-printing phases and the result of the 3D printing of one of the first prototypes of the facial envelope.



Figure 1 From top to bottom and from left to right: succession of stages of processing of the external shell of the face mask obtained by means of 3D printing.

A key aspect of the respirator is its droplet filtering functionality. As anticipated, the AG-47 SmartMask respirator has filters equipped with class N95 filtering capacity which, however, are also equipped with an advanced "active" filtration function, aimed at killing viruses in a permanent, autonomous and constant way.

2.1.2 Active filter

The AG-47 SmartMask respirator is a personal protective equipment (PPE) intended both specifically for health workers (doctors, nurses, stretcher bearers, 118 drivers, etc.) and for civilian and military users operating in areas with risk, as well as to ordinary citizens. Active filtration is carried out and obtained by an electro-heated filter and brought to a minimum temperature of 38° C. It is based on the thermolability principle presented by the SARS-CoV virus [9] which, with a good approximation, is comparable to the profile of the pathogen currently responsible for the pandemic in progress, as it belongs to the same family. The filtering action takes advantage of the action of the electric current passing through the filter, helping to break down the viral load by producing a micro electric discharge on the pathogen that should be deposited on the surface of the conducting wire constituting the active filter [10]. The AG-47 SmartMask respirator can use the same filter up to sixty days from first use; the respirator therefore does not belong to the "disposable" APVR category and therefore has an extremely limited environmental impact. The so-called "active" action of the filter naturally adds to that of the "passive" type carried out by the non-woven fabric (TnT) materials of which the common surgical masks are made. The double "active-passive" functionality of which the filter of the AG-47 SmartMask is equipped is obtained by inserting a layer of a special conductive fabric suitably spun (active filtering zone) between the two surface layers in TnT (passive filtering zone).

The active function of the mask is ensured by a low voltage power supply which must guarantee the maintenance of the thermal requirement established for a significant reduction of the viral load. In this regard, it is necessary to specify that at a temperature of 38° C and a Relative Humidity of 80-90% (RH) there is a significant decrease, up to 14 times, in the percentage of a standard infected culture dose (TCID₅₀) over a period of time. of 24h. A further increase in abatement, equal to 24.5 times, is obtained with 95% RH at 38° C, again in a time of 24h. Note how the RH values are almost similar to those of human breath and therefore replicable within the facial containment cavity of the respirator. Finally, SARS-CoV is completely eliminated at 56° C in 15 minutes [9]. This result is the basis of the self-sanitizing function of the respirator that was described above. This feature allows the entire filtering system of the respirator to be automatically sanitized, without the need for any intervention by the user, simply by connecting the respirator to an electrical transformer that delivers direct current at low voltage. The sanitization process, during which the lithium-ion batteries that power the sensing and control electronics of the device are also recharged, is coordinated entirely by the device's microcontroller unit (MCU). This process is designed to be carried out, ideally, at the end of a prolonged session of use, such as a work shift (8h-10h, for example) and lasts about 15 minutes. At the end of the self-sanitization cycle, the AG-47 SmartMask can be reused in complete safety. The device firmware keeps track of the number of cycles of use and informs the user about the need to replace the filters after an appropriate number of sanitizing cycles. The filters have a useful life of approximately 120 complete cycles of use). The electrical structure of the active filter is shown in the figure 2.

Detail structure of the conductive active filter used in the air inlet and outlet of the AG-47 SmartMask respirator are visible in the Figure 2. In the image it is possible to detect the partitioning of the conductor in different spinning areas, each representing a circuit element subjected to an electrical potential difference.

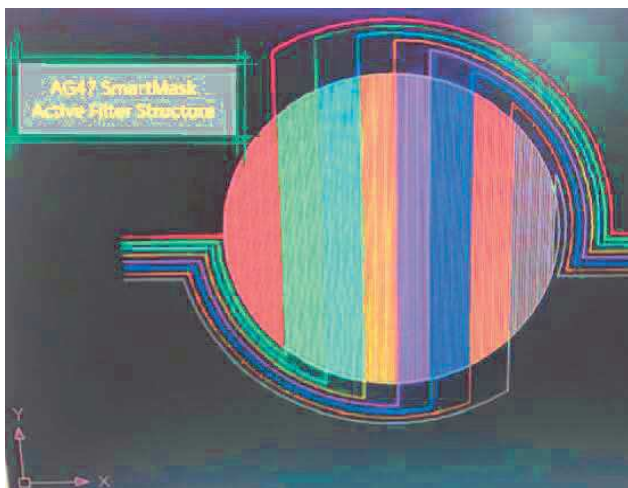


Figure 2 Partitioning of the conductor in different spinning areas.

The active filter (conductor circuit) has been successfully subjected to a series of thermo-electrical stress tests to verify its robustness and identify possible operating anomalies. At the same time, the values of the current intensity, voltage and temperature of the system were measured to qualify its compliance with operational, functional and sensory requirements. The thermal regime maintained at a constant minimum temperature of 38° C contributes to a significant reduction in the viral load contained in the humid air of the breath of an infected person. In particular, at this temperature and at a Relative Humidity of 80-90% RH there is a significant decrease, up to 14 times, in the percentage of a standard infected culture dose (TCID₅₀) in a time of 24h. A further increase in abatement, equal to 24.5 times, is obtained with 95% RH at 38° C, again in a time of 24h. In the event that the user wishes to opt for active protection, he can activate this function in the respirator. The maintenance of the active filtering function is ensured by a direct current power supply generated by an external and replaceable battery-pack, which can be connected to the filter by means of a special power connector, which guarantees a charge of no less than 4 hours of autonomy. The decrease in temperature below this threshold is signalled by the lighting of a red LED located in the side body of the respirator. A green lit LED, also located in the side body of the respirator, instead signals the maintenance of the constant value of 38° C, that is the "active" state of the internal filter. A power cable connects the external battery-pack faceplate. The user wears the respirator connected to the battery-pack without perceiving the heat of the temperature (38° C) on the skin of the face and in any case without feeling general discomfort caused by the same. The AG-47 SmartMask respirator even undergoes complete self-sanitation of the entire filter surface at a minimum temperature of 56° C, during the process described above. Considering the possible physical discomfort associated with the heat generated at this temperature, the respirator must obviously not be worn by the user at this stage; it is instead connected to the electricity network (220 V) using the same cable described in the previous paragraph but with the use of a low voltage, direct current transformer. The lighting of the green LED, already described above, will signal the achievement of the target temperature, warning the user that the device is fully sanitized and ready for use. The expected time for the self-disinfection phase is about 20 minutes. Subsequently, the user can wear the fully sanitized mask. The filtering layers forming part of the AG-47 respirator are superimposed on each other so that the active filtering layer is in the intermediate position between the two passive layers, one of which is external (ambient side) and the other internal (face side). The assembly of three layers is made with simple stitching along the edges; all in accordance with the UNI_EN_14683 standard, which does not provide for the drilling of the filter area with a needle. The active layer is thermally mapped by thermal sensors and thermostated by an automatic controller.

The thermal sensors are integrated in the electro-heated fabric, while the control circuitry occupies a marginal position that is on the edge of the mask, where the positioning of the power socket is practical and feasible. Of course, this position does not affect the filtering area and does not cause discomfort during use. Such a circuit has the following advantages, significant for the purpose of practicality and safety of use: very high efficiency; maximum degree of miniaturization; low electromagnetic emissions; robustness, or dimensioning with a current at least double that required by the heating element; minimum number of components necessary for the realization; adaptability to any type of wire weft: even in the event of variations it would retain its validity. The deposition technology using artificial dry fiber needles (stitching) usually used and available to the proposing subject and his team, allows us to equip ourselves with reliable industrial capabilities aimed at mass production of this product. The 3D Stitching technology adopted consists in the continuous deposition of natural (hemp) and non-natural (carbon, silicon, Kevlar, copper, silver, gold, aluminum, silica, etc.) dry fibers using needles.

2.2 SELECTED FUNCTIONAL VARIABLES

Here we described the functional variables selected on the basis of their diagnostic value for COVID-19 infection and which can be acquired with enabling technologies /devices that were integrated into our wearable mask device. These functional variables have been selected as fundamental parameters to design the sensor system of the AG-47 SmartMask respirator which allows to acquire critical information concerning respiratory, cardiocirculatory and thermoregulatory systems.

2.2.1 Respiratory system

2.2.1.1 Breathing pattern

From a chronotropic way, a respiratory cycle is characterized by the inspiratory time (T_I) followed by the expiratory one (T_E) and a total time of the respiratory cycle (T_{TOT}) which latter is obtained by summing the first two respiratory times of a given respiratory cycle:

$$T_{TOT} = T_I + T_E \quad (1)$$

The graph in figure 3 represents the thermographic oscillation relating to a breath extrapolated from a sequence of quiet breaths in an adult and healthy subject. It can be observed that, by drawing an ideal segment that intercepts the vertex of the curve parallel to the ordinate axis, the thermogram can be divided into two successive temporal phases, the first of which begins with the minimum point on the left up to the maximum point which follows it, or vertex, identifying on the abscissa axis the expiratory time T_E of a given spirogram since, as is known, the temperature of the air during its expulsion in the expiratory phase is generally higher than the external one since it derives from the internal temperature of the body.

The second temporal phase starts right from the vertex and ends with the minimum point that follows it to the right, identifying on the abscissa axis the inspiratory time T_I of the next breath. In this case the heat of the exhaled air tends to be dispersed in the environment during the expiratory pause so that, during the following inspiration, its temperature progressively decreases. In the figure, the lower double arrow highlights the T_{TOT} or the total time of the considered breathing cycle.

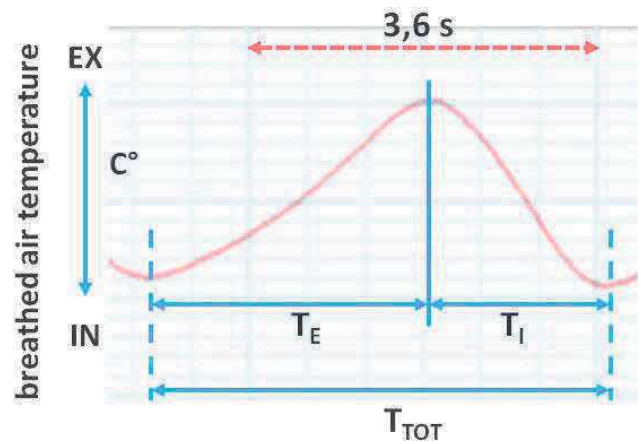


Figure 3 Graph is a single breath thermogram for Expiratory (T_E) and Inspiratory (T_I) phases.

What clearly appears from this figure is that the temporal sequence of the inspiratory and expiratory phases of the thermogram is exactly reciprocal with respect to that of the coincident tidal volume of the breathed air. In fact, during exhalation the quantity of air emitted to the outside decreases progressively while the quantity of heat of the expelled air has an opposite behaviour as it progressively increases. As regards the subsequent inspiratory phase, the relationship of quantitative reciprocity, respectively of the heat and of the air introduced into the lung from the outside, is maintained even if with inverted signs as while the inhaled air volume increases its temperature decreases.

But that is a sensorial experience that each of us can do very simply by placing the palm of a hand near the nose, he will perceive that the exhaled air is warmer than the ambient air but that this sensation will change abruptly at the time of the change phase towards inspiration whose beginning is characterized by a significant lowering of temperature.

On the basis of the above, what therefore can be safely stated is that the duration of the T_I and T_E and therefore of the T_{TOT} , can be calculated thanks to the simple acquisition of a respiratory thermogram whose sensor is placed inside the face mask and in proximity of the respiratory orifices. From this observation it follows that, in this way, it is possible to measure the temporal breathing pattern of a subject without having to connect it to cluttered pneumotachometric devices which, however, could never be used for our facial device.

2.2.1.2 Respiratory time intervals

Among the T_I and the T_E breathing intervals, especially the former has diagnostic value for the context we are dealing with here. In fact, the T_I is an expression of the extent of the excitatory nervous output through the phrenic nerve on the diaphragm (this is the most important inspiratory muscle responsible for about 80% of the air introduced into the lungs with a breath). This evidence is reported by experiments on anesthetized animal preparations [11] in which it was observed that during the electrical stimulation of the sciatic nerve trunk, surgically detached from the soleus and both the lateral and medial gastrocnemius muscles, i.e. the so called *triceps surae* muscle, and whose frequency simulated the rhythmic contraction of the calf during walking, the T_I was instantly reduced by about 20%, thus inducing an increase in respiratory frequency (F_R) of exclusively nervous origin. Furthermore, experiments on healthy subjects who were forced to passive rotation of the ankle joint, producing alternations of dorsal and plantar flexions of the foot, showed an instantaneous and significant reduction of the T_I (-7%) [12], from which also in this case, an increase of the F_R of exclusively nervous origin occurred. It is therefore possible to hypothesize that alterations of this precise breathing control mechanism on an exclusively nerve basis being integrated in a broad spectrum of cortico-brainstem and spinal structures, may occur caused by invasion of COVID-19 in the central nervous system through retrograde axonal transport in the peripheral nerves [13]. In this case, the phrenic nerve that connects brainstem structures with the inspiratory musculature which, for obvious anatomical reasons, appears to be concomitant with the alveolar structures within which COVID-19 infection is established. It can therefore be reasonably assumed that the prodromes of these conditions of early COVID-19 brain distress could be diagnosed by a breath-by-breath analysis of the T_I .

2.2.1.3 Respiratory rate per minute

It is easy to acquire the breath-by-breath value of the respiratory rate, or respiratory frequency (F_R), of a subject engaged in a working performance, on the basis of the relationship:

$$F_R = \frac{1}{T_{TOT}} \quad (2)$$

and then report it to the number of breaths per minute:

$$F_R \text{ min} = \frac{60}{\left[\frac{1}{\left(\frac{1}{T_{TOT}} \right)} \right]} \quad (3)$$

An increase in the F_R in a subject not engaged in sustained physical activity, as may be the case of the healthcare professionals engaged in their specific activities with COVID-19 patients or in other work activities at risk of infection, among other possible causes it could represent a compensatory response to insufficient respiratory tidal volume (V_T) due to a possible restrictive damage of lungs that prevents normal inspiratory expansion.

This may be the case of consolidations of the lung parenchyma caused by thickening of the wall of the alveoli and their filling with proteinaceous liquid whose computed tomography images are of the "ground-glass opacification" type, characteristic of acute and severe respiratory complications of infection with COVID-19 [14].

2.2.1.4 Inspiratory duty cycle

The T_I takes on a further functional value ($T_{I\text{-}funct}$) when it is related to the entire period of the breathing cycle:

$$T_{I\text{-}funct} = \frac{T_I}{T_{TOT}} \quad (4)$$

This ratio is also known as the inspiratory duty cycle (IDC) of the work of the inspiratory muscles. It has been observed that a decrease in IDC is accompanied by a decrease in aerobic capacity due to reducing the inspiratory fraction of oxygen (ΔFO_2), i.e. the difference between the oxygen fraction of the alveolar air at end inspiration ($F_I O_2$) and that at end expiration ($F_E O_2$) [14]. The reduction of ΔFO_2 , indirectly detected by a decrease in T_I / T_{TOT} , is configured as a net reduction of the partial pressure of oxygen in the arterial blood or as an hypoxic hypoxia probably caused by a limit of diffusion of this gas from the alveoli to the lungs capillaries because of decrease in pulmonary ventilation linked to restrictive respiratory damage from COVID-19.

Furthermore, as suggested by recent clinical observations [15], the value of the LDCO (lung diffusion capacity of the carbon monoxide) between alveoli and pulmonary capillaries, is significantly reduced in patients affected by COVID-19 [16], and this implied a decrease in speed transit of oxygen from the lungs to the blood, worsening the condition of hypoxic hypoxia due to a limitation of pulmonary ventilation. But this arterial hypoxia could also be supported by a limit to the pulmonary diffusion of oxygen due to a decrease in blood flow in the pulmonary capillaries because of a decrease in cardiac output.

In this regard, the case cited by the National Health Commission of China [17] concerning patients who presented to the general practitioner with cardiovascular symptoms as tachycardia, heart palpitations and chest tightness, but without respiratory symptoms, cough or fever, is alarming because only very late were they diagnosed the COVID-19 but, in the meantime, irreversible myocardial damage had developed. It is important to emphasize that the clinical observation referred above reinforces the need to acquire early not only respiratory but also cardio-circulatory indicators for possible cardiovascular damage in those professional workers involved in the care of patients with COVID-19 infection.

2.2.1.5 Respiratory tidal volume

The respiratory tidal volume (V_T) represents the amount of air that enters and leaves the lungs with each quiet breath.

It is on average about 400-500 mL and is generated by an expansion of the rib cage, due to the activation of the inspiratory muscles (diaphragm and external intercostal muscles) which generate a depression (-1 mmHg) with

respect to the external air, from which an influx of air into the lungs that lasts until the intrapulmonary pressure balances with that of the external air. At this point the brainstem clock inhibits the activity of the inspiring neurons and the muscles are released. The thoraco-pulmonary structures, which have accumulated elastic energy due to their stretching during inspiration, at this point release it in the form of concentric pressure on the intrapulmonary air whose pressure increases compared to that of the external air (+ 1 mmHg), generating the expiratory outflow which ends when the two pressures: internal and external, rebalance themselves after having emitted a volume of air equivalent to the inspiratory one. The quiet exhalation is therefore a completely passive breathing act as no muscle energy is spent on its implementation. The sensors for the biophysical variables that can be acquired with the AG-47 SmartMask instrumented face mask do not include sensors for the volume variation of the breathed air. However, it is possible to indirectly derive the V_T thanks to its linear and positive correlation with the T_I [18]. On this basis, in healthy subjects who breathed ambient air while sitting in conditions of physical and mental rest, the T_I and the inspiratory tidal volume V_T were measured on three consecutive respiratory cycles. The linear regression equation between these two variables was then calculated with the T_I as the independent variable and the inspiratory V_T as the dependent variable:

$$V_{T-insp} = (106 \times T_I) + 275 \quad (5)$$

The linear regression equation (5) was found to be statistically significant ($P < 0.01$) so that for each unit variation of the T_I , i.e. ± 1 s, the V_{T-insp} increased or decreased by 106 mL. The possibility of indirectly calculating the V_{T-insp} through its regression on the T_I allows to acquire this very important spirometric variable.

2.2.1.6 Pulmonary ventilation

The indirect acquisition of the value of the V_{T-insp} , allows above all to have a reliable estimate of the most important respiratory variable: the inspiratory pulmonary ventilation per minute (V_{P-insp}) obtainable as a product between the V_{T-insp} and the F_R , i.e. the quantity of air that the lungs of the worker under examination inhale in one minute:

$$V_{P-insp} = V_{T-insp} \times F_R \quad (6)$$

Equation (6) allows to estimate, breath by breath, the mode of interaction between chronotropic control mechanisms (the F_R) and inotropic control mechanisms (the V_{T-insp}) of pulmonary respiration integrated in the V_{P-insp} . The whole of these three variables of the respiratory pattern makes it possible to verify which of the two control modes could be prevailing over the other and this, for example in the healthcare worker involved in the care of COVID 19 patients, can be of considerable importance. In fact, an excessive increase of the V_{P-insp} in conditions of static activity, and therefore not justified by increases in energy/oxygen demand, may indicate a suffering of the

mesencephalic structures that control respiration with particular reference to the pneumotaxic center. Otherwise, an excessive increase in F_R may indicate a condition of hypercapnia in the arterial blood (the partial pressure of arterial CO_2 greater than 40 mmHg) which could depend on the reduced diffusion of this gas from the pulmonary capillary to the alveolus due to due to impairments in the mechanisms of diffusion itself or in the perfusion of blood in the pulmonary capillaries. However, an abnormal hyperventilation at rest, on a predominantly tachypnoic /dyspnoic basis, can be a quantifiable index of acute respiratory distress symptoms (ARDS) [19] which should lead to refer the health worker (or other) to subsequent checks of positivity or not for COVID 19 infection.

2.2.1.7 End tidal carbon dioxide

In addition to the introduction of oxygen into the arterial blood during inspiration, the other important function of pulmonary ventilation is to expel carbon dioxide (CO_2) from the venous blood that comes into contact with the alveolar epithelium during exhalation. This occurs thanks to the partial pressure gradient of this gas ($\Delta P_p CO_2$) which is established between the venous capillary compartment and the alveolar compartment. In this way, pulmonary ventilation acts as a buffer for the increasing metabolic acidity due to the biochemical reactions of oxidation of the substrates, especially carbohydrates and lipids, which take place at the mitochondrial level in active cells.

In short, sugars and fats substrates are reduced to H_2O and CO_2 molecules. The latter, thanks to the carbonic anhydrase enzymatic complex present in the blood, is re-aggregated with the H_2O forming carbonic acid (H_2CO_3) which, however, being a weak acid, dissociates releasing a protons (H^+), from which there is a reduction of blood pH , and forming bicarbonate ions (HCO_3^-). As is known, blood pH must be kept within a narrow range, between 7.35 and 7.45, to ensure the proper functioning of metabolic processes and the release of the right amount of oxygen to the tissues. Normally, the pH omeostasis is maintained since the physically dissolved CO_2 in the venous blood reaches the alveolar capillary circulation where it flows inside the alveoli and from there expelled into the ambient air during the expiratory phase, allowing the pH to remain within physiological values.

Now considering the fact that tachypnea is a major indicator of incipient COVID-19 infection, end-expiratory partial pressure of alveolar carbon dioxide ($ET-P_p CO_2-A$) is expected to decrease, as the hyperventilation underlying this increased respiratory rate is not an adaptive response to an increase in the body's demand for more oxygen to meet the increased need for adenosine-triphosphate. In fact, by increasing the amount of CO_2 -poor air that pours into the alveoli while the venous blood dissolved CO_2 partial pressure ($P_p CO_2-v$) does not change, the result would be a rapid decrease in the $ET-P_p CO_2-A$. In a respiratory test, healthy adult male subject voluntarily produce a forced hyperventilation (at least doubled compared to the resting condition) for 10 s obtained by keeping the V_T constant and

therefore characterized only by the increase in R_F [20]. Results showed that, when R_F went from 10 breaths/min to about 25 breaths/min, the breath-by-breath trend of end-expiratory $ET-P_pCO_2-A$ peak was visibly reduced. The aforementioned finding, however well known to clinicians and respiratory physiologists [21], [22], highlights however the critical value that the condition of relative respiratory hypocapnia observed in conditions of involuntary tachypnea as the latter, not being accompanied by an alveolar normocapnia, unequivocally reinforces the risk of a condition of respiratory distress caused by possible damage to ventilation and/or lung perfusion that could act as prodromes of lung damage from infection with COVID-19.

2.2.1.8 Fits of coughing

From the pressure sensor installed inside the mask which detects the intra-face mask pressure oscillations, it can be assessed the possible occurring coughing fit by the size and excessive amplitude of the pressure of the expired air. Coughing is due to a nervous reflexes which gives rise to an energetic contraction of the inspiratory muscles followed by a rapid expiration with closure of the glottal rim. This is followed by a reopening of the glottal rim accompanied by a sound vibration followed by an elevation of the soft palate which occludes the nose-pharynx structure. Since the occurrence of repeated bouts of coughing is one of the prodromal signs of an incipient COVID-19 infection, their detection reinforce the indicators to be taken into account for the possible COVID-19 disease in progress.

2.2.2 Cardiocirculatory system

2.2.2.1 Heart rate

The cardiac output per minute (C_O) is the volume of blood ejected in one minute from the left ventricle into the aorta artery from which it is then distributed to all organs and systems, is finely regulated in the domain of the force of contraction of the heart (inotropic control), in the time domain of duration of heart contraction (chronotropic control) [23]. However, the peripheral vessel hydraulic resistance due to their vasodilation /vasoconstriction status, is the third element that conditions the distribution of C_O in the different vascular districts [24].

The main cardiodynamic variable in the inotropic domain is the systolic ejection volume (also called stroke volume: S_V , i.e. the amount of blood that, beat by beat, is ejected from the left ventricle into the aorta artery, on which the systolic and diastolic blood pressure depend. The main cardiodynamic variable in the chronotropic domain is instead the heart rate (HR) on which the alternation between contraction and relaxation of the myocardial muscles depends, i.e. the succession between cardiac systole and diastole, and is measured in beats per minute and is:

$$HR = \frac{60}{\left(\frac{1}{T_{cycle}}\right)} = \frac{cycles}{min} \quad (7)$$

where T_{cycle} is the time interval between one peak of the R wave of the ECG and the next. C_O depends on both inotropic and chronotropic variables as follows:

$$CO = V_S \times HR \quad (8)$$

Although C_O is the most important cardiodynamic variable since the supply of oxygen per minute to the body's tissues depends on this variable, it is not easy to measure since the measurement of one of its two generating variables: the V_S , as a rule takes place in highly invasive way and in specialized clinical structures such as the units of intensive cardiac care. Because of this, for diagnostic purposes, the V_S is surrogated by the simpler measure of the mean arterial blood pressure (M_{ABP}), for which an indirect, but clinically effective estimate of the C_O is obtained based on the observation of the reciprocal trend of M_{ABP} and HR . In general, in steady state conditions of energy expenditure, the C_O tends to remain constant so, based on equation (8), incidental beats by beats increases of M_{ABP} are instantly compensated by corresponding decreases in HR and vice versa. Unfortunately, due to the ergonomic needs highlighted in the previous chapter, it is not functional to apply additional sensory devices that are not in close spatial relationship with the instrumented face mask proposed here, such as installing a bracelet or ring sensor in one finger for the M_{ABP} measurement. On the contrary, through a short wired extension of the face mask, like an earring sensor suitable for the HR beat-by-beat acquisition is integrated into the lobe of an ear. On the other hand, in conditions of mental engagement with periodic light physical activity, such as that which can be assumed in health workers engaged with COVID-19 patients, but also in agricultural processing industry workers engaged along the package chain of horticultural products, the V_S and therefore the M_{ABP} , practically do not change. In fact, it was observed that in healthy subjects applied on a mental test of not negligible involvement (solving mathematical expressions in rapid succession) while physical activity consisted in writing the result on a keyboard, the C_O increased by about 25% compared to a task of physical and mental rest, but this increase was almost totally supported by an increase in HR (+ 19%) with no significant V_S changes [25].

Therefore, it is reasonable to believe that the beat-by-beat adjustments of the CO, necessary for the adaptation of the oxidative energy support to the activity of these health workers or similar ones, concerning the locomotor dynamics could be almost entirely carried out in the chronotropic context or through compensatory variations of the HR . However, if we take into account what has already been explained above regarding the recent observation by the "National Health Commission of China" [17] in which it is reported that in subjects with only cardiologic symptoms but no respiratory symptoms there had been a serious delay in the diagnosis of COVID-19 and, due to which, irreversible cardiovascular damage was found, then it is still strategic to be able to acquire the HR beat by beat through

the AG-47 individual safety face mask for workers engaged in jobs which carry a high risk of COVID-19 infection. In fact, abnormal periods of excessive bradycardia or tachycardia or even arrhythmias of various type. can be the prodromes of a more serious myocardial damage from corona virus even in the absence of respiratory symptoms and hyperthermia.

2.2.2.2 Heart sinus node arrhythmia

The atrial Bainbridge reflex [26] give rise to a cyclic or sinus arrhythmia (HS_{arrh}), resulting in peaks of relative increase in HR , due to the excitation of mechanoreceptors located inside the right atrium. During inspiration this cardiac chamber increases its tele-diastolic blood volume and the own mechanoreceptors project excitatory information, on a noradrenergic basis, to the bulbar chronotropic control centres. Consequently, these centres increase the excitability of the atrial sinus node from which a tachycardia occurs. This increase in HR allows blood to be emptied more quickly from the atrium to the right ventricle in diastole. In the subsequent ventricular systole, the surplus of blood acquired by the right ventricle flows into the left ventricle and therefore into the aortic arch, exciting the baroreceptors located inside it, from which inhibitory impulses depart, on a cholinergic basis, towards the same bulbar centres of chronotropic control and from these, through vagal-cholinergic projections, an inhibition of its excitability is superimposed on the atrial sinus node. It is likely that, in conditions of prodromes of myocardial distress, this ortho-parasympathetic balance of heart rate could be significantly altered if not completely unregulated, and this can represent a very sensitive indicator of incipient myocardial suffering from COVID-19.

2.2.2.3 Percentage of oxygen saturation of the haemoglobin

Hypoxic hypoxia of arterial blood, due to excessively limited alveolar ventilation or/and capillary perfusion of the lungs as a complication from infection with COVID-19, must absolutely be detected as early as possible, under penalty of tissue damage especially in the brain and heart. Practically, when the partial pressure of oxygen in arterial blood (P_{PO_2-a}) falls below 100 mmHg, haemoglobin does not bind totally to oxygen as its chemical affinity for this respiratory gas is directly proportional to the P_{PO_2-a} . For this reason, when this blood is not totally saturated with oxygen, when it reaches the tissues its oxygen content may not be sufficient to meet the organs demand for this gas.

2.2.3 Termoregulatory System

Since it has been observed [27] that over 80% of cases of infection with COVID-19 have fever with values between 38° C and 39° C as a prodromal symptom, the instrumented face mask AG-47 has been also equipped with a continuous body temperature detection system. Taking into account the ergonomic limits imposed by the project which aim to engage, for the set of clinical variables to be provided by the AG-47 device, only the lower part of the face with an extension of proximity to an ear connected to the mask

wirelessly, and also considering that the external acoustic meatus of an ear can act as a transceiver peripheral of a mobile telephone, a micro temperature sensor has been installed on this, as proximal as possible to the tympanic membrane. In fact, the measurement of body temperature through the tympanic detection is comparable to the measurements obtained at the oral or rectal level [28].

2.3 MASK SENSORS

The physiological studies carried out, which represent the physiological bases of the project, have been reported in the previous paragraphs and the types of quantities observed, their characteristics, the respective correlations and the types of sensors used to acquire them have been illustrated. The data acquisition process carried out by each sensor in the AG-47 SmartMask respirator is placed under the direct coordination of the device's control electronics. The main element of the electronic control system of the device consists of a MCU which combines high computational performances with extremely low energy consumption levels. By exploiting these characteristics of the main microcontroller of the device and making a pervasive use of power saving algorithms together with wake-on techniques based on external events (detection of signal spikes, hardware watchdog timers and so on) it was possible to combine the performance of relevant computational tasks, relating to the analysis and storage of the acquired signals, with a minimum operating time sufficient to guarantee continuous use of the device for the duration of a typical work shift (8-10 hours), without the need for carry out recharges of the on-board power system (lithium-ion batteries). The duration, frequency and characteristics of each sampling event carried out by each sensor included in the supply of the AG-47 SmartMask respirators are directly controlled by the main MCU and can be configured via software, by means of direct upload of the configuration into the device firmware or through modifications that can be made using the command and control protocol supported by making use of the wireless connectivity in the Bluetooth standard. Changes to the device configuration parameters, therefore, can be transmitted from the AG-47 RTP telemedicine center via direct Bluetooth connection (in the case of completely in-house scenarios) or via the control application operating on mobile devices (remote scenarios in-cloud). Based on the configuration parameters present in the firmware or received from external systems, the MCU performs an orchestration of the sampling sessions of each sensor. The data sampled from each sensor supplied with the respirator is acquired by the main MCU which carries out an analysis in real time. The purpose of the first level of analysis is both to filter the signal to reduce the disturbances present, thus increasing the Signal-to-Noise Ratio (SNR), and to extract features of interest. As far as filtering is concerned, it is necessary to illustrate how, during the development phases of the project, a preliminary study was carried out during which a large number of traces relating to each type of quantity monitored by each sensor present in the respirator were acquired.

These plots were used to develop models of Newtonian reference dynamics systems that are used to filter each signal by means of extended Kalman filters, in order to obtain an optimal estimate of the observed quantities.

The signals thus filtered are subsequently processed by a features extraction module which performs a segmentation by means of predetermined or dynamically adapted confidence intervals, a morphological analysis, a search for local maximum and minimum points and an extraction of inflection points, in order to identify the features of interest present in each segment of each signal. At the end of the segmentation and features extraction process, the MCU proceeds to classify the recognized features to determine the physiological quantities of interest, as described in the previous paragraphs of the manuscript.

Thus, for example, the classification of the barographic, thermographic and hygrographic curves will lead to the identification of respiratory acts, tussigenic events or sneezing. During the feature classification phase, the MCU carries out a further control task, applying consensus algorithms to the detected data, in order to be able to promptly identify any drift and malfunctions of the device sensors.

The consensus algorithms applied mainly focus on consent to the average and are implemented by means of counters contained in special data structures, allocated for each type of data detected on each sensor, which are dynamically updated during the time analysis carried out on these signals. Thanks to this control system, the MCU of the device can quickly assess the state of coherence of the sensors and the onset of any deviation phenomena or malfunction. However, the structure of the signal acquisition system of the AG-47 SmartMask respirator has been designed with maximum flexibility, to support different use scenarios and different product lines, suitable for multiple market targets.

Therefore, although the minimum configuration expected for the respirator contains the sensors described earlier in the text (a thermo-hygrobarometric and a CO₂ sensors inside the mask, an intraural thermal sensor and an earlobe pulse oximetry/heart rate sensor), the device can be equipped with a greater number of sensors of each type.

As an example, the following figure shows the location of the main sensors present in the AG-47 SmartMask respirators. In the images in figure 4 it's possible to see renderings of the three-dimensional design of the AG-47 SmartMask respirator in a configuration that provides for a minimum replication level (equal to 1) as regards the thermo-hygrobarometric-CO₂% sensors present in the facial containment cavity of the mask) but a higher replication level, equal to 2, relative to intraural thermal sensors and pulse oximetry-HR sensors for the ear lobe (sensors positions highlighted in red).

The control electronics and designs allow the use of 1, 3 or 5 thermo-hygrobarometric-CO₂% sensors inside the facial containment cavity of the mask in combination with one or two intraural thermal sensors and ear lobe pulse oximetry.



Figure 4 Different visual angles of the mask internal surface (the positions of the sensors are highlighted in red).

In the event that in a given respirator production configuration there are replication factors greater than 1, for any of the types of sensors supplied, the MCU will be able to apply, during the consent verification phase just described, complete algorithms for perform Fault Detection and Isolation (FDI) actions on the sensors belonging to the group considered. The analysis of data from multiple sensors with these algorithms makes it possible to determine any malfunctions with greater accuracy than the sole use of data from different types of sensors. Furthermore, as regards the thermo-hygrobarometric sensors positioned inside the facial cavity of the mask, a replication factor greater than 1 allows to obtain a real mapping of the quantities observed over time in different points of the internal surface of the facial mask. Finally, in the configurations equipped with replication levels higher than 1 for any type of sensor, the MCU, in the case of the detection of malfunction events of a sensor belonging to this type, will be able to selectively isolate the malfunctioning sensor and in any case guarantee the correct operation of the sensor device using only the remaining sensors of the same type. The dislocation of the thermo-hygrobarometric-CO₂% sensors under the internal surface of the facial containment chamber of the respirator in scenarios with 1, 3 or 5 different sensors was determined using computational fluid dynamics simulations, then also validated experimentally, thanks to which it was possible to identify the most suitable positions to capture the information necessary to accurately construct the environmental scenario present inside the mask during its use. Once the task of classifying the detected features has also been completed, the MCU can proceed to compress the available data and store and/or transmit them in three distinct ways: local storage, partial transmission and complete transmission of all signals and/or related feature points and/or the quantities derived from them. Data compression takes place as a preparatory action for subsequent storage and /or transmission stages, making use of highly efficient proprietary algorithms, both lossy and lossless, which have been developed by exploiting domain knowledge and the Newtonian dynamic models of the observed signals, described above. The compressed data, by way of example, can then be stored in the local storage area of the respirator control electronics in full (i.e. in the form of sampled signals, feature points and diagnostic metadata) and, at the same time, only the diagnostic metadata will be able to be transmitted to the command and control application that implements the user interface on mobile devices.

The different possible combinations of types of data stored and/or transmitted obviously correspond to different levels of energy consumed to perform these operations, which range from a maximum consumption for the storage and transmission of all sampled data, feature points and diagnostic metadata to external devices, up to a minimum energy consumption for the scenario that only provides for the local storage of diagnostic data only. The MCU of the device supports the possibility of dynamically varying the storage and transmission strategies of the acquired data, thus making it possible to modulate the power consumption of the device, for example, in the case of low power availability necessary and the need for unexpected extension of the use sessions.

2.4 EAR WIRELESS MOBILE

The monitoring functions of the user's physiological parameters represent one of the main health prevention and control capabilities offered by the device. However, the AG-47 platform and, in particular, the AG-47 SmartMask respirator, make use of an integrated approach to personal and community safety, which makes use of multiple levels of protection to preserve health. This integrated approach, as already briefly illustrated in the previous paragraphs, is also based on the integration of contact tracing functions that the respirator is equipped with, by means of which it is possible to know the network of contacts of a potentially infected person and to promptly alert all subjects who are at risk of contagion. A further set of features designed for the integrated approach to health protection consists of a set of tools that facilitate the use of the respirator in the workplace even for long periods of time, encouraging its use and reducing the risk of infections due to self-contamination. These two sets of functions will be detailed below which, together with the physiological monitoring and early diagnosis capabilities of the system, constitute a highly effective preventive device in respiratory disease scenarios. Both sets of features presented by the AG-47 SmartMask revolve around its ability to communicate through short-range wireless networks, making use of the Bluetooth standard and in particular version 4.0 (with Low Energy - LE extension) of this standard. Bluetooth connectivity is guaranteed by the availability, within the electronics supplied with each unit, of a low consumption, high miniaturization BT 4.0LE certified Bluetooth radio module with integrated antenna that implements different communication profiles provided for by the standard. The radio integrated in the respirators is coordinated by the main MCU (MicroController Unit) present inside the SoC (System on Chip) with the function of command and control of the entire device. The main features supported by this subsystem of the AG-47 SmartMask are described below.

2.4.1 Contact Tracing capabilities

The first and fundamental functionality supported by the wireless communication system of the AG-47 SmartMask respirators is the ability to constantly monitor the surrounding environment to check for the presence of

devices equipped with a Bluetooth radio system, active in the vicinity of the respirator. Structure of the standard identifier BD_ADDRESS. The less significant 24 bits are divided into the Non significant Address Part (NAP), used in the synchronization activity of the frames during the frequency hopping phases and in the Upper Address Part (UAP), used in the seeding of the protocol. Together these two fields form the Organizationally Unique Identifier (OUI), assigned by the Institute of Electrical and Electronics Engineers (IEEE) to each Bluetooth hardware manufacturer, the remaining most significant 24 bits form the Lower Address Part (LAP), assigned by the device manufacturer. This functionality is implemented through a series of scans of the radio baseband provided in the Bluetooth standard (from 2.4 to 2.4835 GHz) to detect the presence of active devices, making use of the same standard. Each Bluetooth device is identified through a unique code predefined by the device manufacturer (called Bluetooth Address, BD_ADDRESS), consisting of 48bit, the format of which is shown in the following 5.

The set of data that make up the BD_ADDR fields therefore represent a unique identifier, for each Bluetooth device, which can be used to track contacts in basic operating mode, provided for by the standard itself. However, broadcasting a unique identifier per device poses privacy concerns that cannot be ignored. For this reason, the Bluetooth stack implemented on latest generation devices (in particular on smartphones and tablets) is increasingly changed dynamically by the device's operating system to make it more difficult to associate with a single physical device. The AG-47 SmartMask respirator also supports this second operating mode, which requires a collaborative inter-device effort to perform tracking activities and which is at a higher protocol level than described for basic operation. This approach is supported by some applications proposed to support contact tracing at national level (eg. "Immuni" App selected for the implementation of this system in Italy) and makes use of specific Application Programming Interfaces (API) recently developed by major manufacturers of mobile operating systems (Google for the Android operating system and Apple for the iOS operating system). Through the use of these technologies, the AG-47 SmartMask respirator can therefore be integrated into wider tracking frameworks, interacting with regional or national data exchange systems.

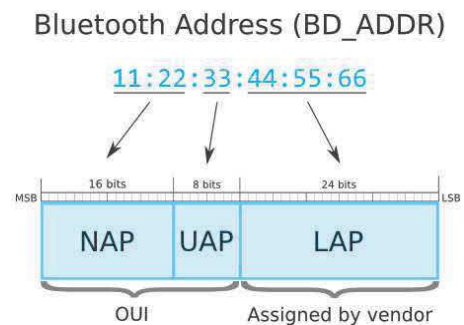


Figure 5 Structure of the standard identifier BD ADDRESS.

However, in some usage scenarios, contact tracking can be done on a strictly local basis. For example, an industrial site can choose to track contacts only with devices enabled within the company and/or only with other AG-47 SmartMask respirators. In this case, the respirator's electronic control system will dynamically generate local identification codes that can be used for contact tracing activities exclusively within the company site. The data related to contact tracing, in this operating mode, are never used outside the company context and are exclusively visible by authorized company personnel. Each respirator AG-47 SmartMask is able to store contact data for over a week of use and can at any time transfer them to the server side of the AG-47 RTP telemedicine platform, according to the methods described later in this paper.

2.4.2 Hands Free Operations Capabilities

The second set of features supported by the short range wireless system based on the Bluetooth standard is related to the possibility of bi-directional transfer of audio signals to and from the AG-47 SmartMask. This functionality is implemented, from a physical point of view, by means of intraural earphones equipped with microphones, capable of reproducing and capturing audio signals. The model structure of this part of the AG-47 SmartMask is shown in the figure 6.

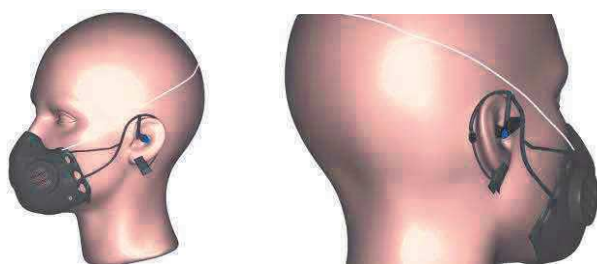


Figure 6 Dummy heads in which the auricular structure of the respirator is visible

The auricular structure of the respirator, as visible in the figure above, also allows the connection to the body of the pulse oximetry + HR sensor and integrates, in the intraural section (not visible in the figure), the tympanic temperature sensor already described above. The ability to acquire, play and transfer audio through the intra-aural headset integrated into the respirator allows us to use the device in hands-free mode, in combination with a smartphone or other mobile device associated with it. In this mode of use, the respirator can be used similarly to a Bluetooth headset, to answer incoming calls received on the smartphone connected to the respirator, without requiring the operator to use his hands to operate the smartphone itself. The respirator's audio acquisition, reproduction and transfer system, however, also interfaces with the SoC that coordinates the command and control functions of the AG-47 SmartMask. Thanks to this interaction and the use of state-of-the-art signal algorithms, the AG-47 SmartMask respirator supports an additional set of advanced features. The respirator control electronics is waiting for particular vocal patterns pronounced by the user.

If the user pronounces a predefined voice pattern, the respirator can activate an intelligent assistant operating in the smartphone connected to it. The AG-47 SmartMask respirator supports the activation of the Google assistant (Google Assistant, for the Android and iOS operating systems) and the Amazon assistant (Alexa Assistant, for the Android and iOS operating systems). Thanks to the hand free and voice activated use of these assistants, the user wearing the respirator will be able to carry out a large number of operations via their smartphone (such as reading and composing e-mails and messages, making telephone calls to contacts on the address book, request information, search the internet, write down notes, events and so on) using only the voice command, without the need to use our own hands. It is clear that this possibility, particularly in view of the more stringent limitation of risks and exposure to contagion, is extremely important to facilitate normal work activities without however increasing the risk of self-contamination of the operators employed. Furthermore, the activities that can be carried out using voice commands, by means of the aforementioned intelligent assistants, are constantly expanding thanks to the availability of APIs through which third parties can integrate new functions and services. However, the AG-47 SmartMask respirator is not limited to a passive role, of mere activation and transfer of audio signals, compared to the voice assistants but, rather, it integrates deeply with them. In fact, customized actions will be developed integrated with these assistants through which the user of the respirator will be able to request, by means of voice commands only, data relating to his own biomedical parameters acquired by means of the sensors of the device, information about the operating status of the device (e.g. residual charge level, temperature and humidity inside the mask, operating temperature of the filter, and so on) and to issue commands to modulate some operating parameters of the respirator itself (e.g. increase/decrease volume level, deactivation of the active filtering function, switching to a low power consumption mode, and so on). In fact, therefore, all the functions relating to the biomedical parameters acquired, the operating status of the respirator and the related configuration parameters will be exposed, accessible and configurable directly through a voice interface, fully operable in hands-free mode, capable of constantly maintaining high level of protection for the user of the device. The AG-47 SmartMask respirator also supports an additional operating mode, in which the short-range wireless communication system is not interfaced directly with a smartphone but with a Bluetooth system.

2.5 INFORMATION & COMMUNICATION TECHNOLOGIES

The wireless communication system making use of the Bluetooth standard with which the AG-47 SmartMask respirators are equipped plays, in addition to what has been illustrated up to this point, an additional functional role. This subsystem, in fact, oversees all the interfacing functions of the respirator with external devices as regards the exchange of data and the sendi

ng of command and control information. As mentioned in the previous paragraphs, the AG-47 SmartMask can interface both with smartphone or tablet class systems and with corporate network infrastructures with support for the Bluetooth standard. In the case of interfacing with mobile devices of the smartphone or tablet class, the respirator is able to communicate with a mobile application that can be installed on Android and iOS operating systems, specially developed for the needs of the project. Once installed, the application scans the AG-47 SmartMask devices that are in the radio range of the device and allows the association of a single respirator. Once associated, the application allows you to monitor in real time all the biomedical and electrical parameters acquired by the respirator, to configure the main operating variables and to issue commands to change the operating status of the respirator itself. The mobile application also has the function of transferring the data detected by the respirator to carry out second-level analyzes, i.e. large-scale statistical analyzes using machine learning techniques, to the telemedicine centre to which the respirator has been associated. The telemedicine centre can be remote, offered in SaaS mode to the target customers of the project or internalized in the corporate ICT infrastructure of a single customer. Finally, the mobile application developed for AG-47 SmartMask respirators, after being installed on mobile devices equipped with a Google or Amazon voice assistant, automatically integrates the functions supported by the respirator with the list of voice activities. made available by the assistants, thus extending their functionality as described earlier.

2.6 EXPERIMENTAL PROTOCOLS

In order to validate the technologies embedded in the anti-COVID-19 instrumented facial respirator AG-47 SmartMask, it have been produced some prototypes to be applied, in the workplace, to the operators of a precision farm in which they were engaged in the horticultural product packaging and package department. These workers, both males and females, carry out work activities characterized by an energy expenditure considered “light”, but which often obliges them to act in groups with obligatorily reduced inter-individual distances.

2.6.1 Work environment and its procedures

The validation and demonstration sessions of the AG-47 platform technology took place at the headquarters of one of the largest companies operating in Italy in the precision agriculture sector, processing and marketing of fruit and vegetables in the Sardinia Region, in the territory of the Municipality of Sestu, in the province of Cagliari. The company headquarters is divided into an industrial warehouse of about 4,500 square meters within which over 30 employees work, assigned to the functions of receiving agricultural products conferred by associated farmers, warehouse logistics, delivery of processed products to the company’s customers and cryopreservation of products in cold rooms.

The entire area of the shed is equipped with a Bluetooth wireless network used for wireless voice control functions made available to logistics operators who, using electric vehicles to move goods, interact with the company system vocally, without having to do use of hands. The platform was installed in a dedicated Kubernetes cluster separated at the network level from the rest of the corporate ICT architecture, which was activated within the pre-existing corporate ICT infrastructure, consisting of a set of 12 physical servers, in which virtual machines are operational (fully virtualized with QEMU-KVM virtualization) necessary for carrying out common business activities. The voice control system at the service of logistics operators has been integrated with the voice control functions of the device directly on the server side of the platform, by interconnecting the AG-47 RTP modules with the Bluetooth network system (see figure 7 and 8).



Figure 7 Two workers engaged in the vegetable packaging supply chain wearing AG47 smart masks.



Figure 8 A worker which wears the AG47 smart mask while driving an electric goods lift truck.

2.6.2 Engaged workers

Among the workers who volunteered to participate in the trial, 27 were enrolled, 15 of whom were male and 12 female. Their mean age was 43 ± 11 years with a weight of 66 ± 13 kg and a height of 1.60 ± 9 cm. Their clinical history showed that none of them were chronically affected by cardio-respiratory pathologies or by endocrine-metabolic syndromes as well as by ear, nose, and throat and haematological pathologies.

2.6.3 Face-mask validation protocol

2.6.3.1 Choice of type and sequence of breathing patterns carried out by the workers

After wearing the AG-47 face mask while staying in their usual work station, each subject breathed quietly (subjectively eupnoic) for 10 min in order to adapt to the device worn; the remote variable acquisition system was then activated by the biomedical sensors embedded inside the face mask while the people breathed quietly for another 3 min; at the end of the third minute the subject performed a sequence of 5 tachypnoic and superficial breaths (thus simulating the condition of COVID-19 dyspnoic breathing), avoiding as much as possible to increase the volume of inspired air (voluntary tachypnea at rest was limited to only 5 breaths to avoid possible situations of cerebral ischemization due to arterial hypocapnia with risk of syncope [29]); at the end of the voluntary tachypnea, recovery of normal quiet respiratory activity for a further 3 min and then voluntarily provoking 3 coughs.

2.6.3.2 Collection, selection and processing of the acquired instrumental data

For each worker tested, the instrumental traces acquired remotely and related to the variations in the time domain of: $t^\circ C$, $U\%$, $Pressure Pasc$ and $CO_2\%$ intra-facial mask, were independently viewed by two experts in bioelectrical signal analysis in order to validate their morphological and dimensional quality, moreover the experts have also viewed the traces of the tympanic temperature ($t^\circ C timp$) and of the ear pulse oximetry + HR ($PO aur$); for each respiratory cycle performed by each subject in the pre-test, test and post-test phases, the dedicated software calculated the values of: F_R , T_I , T_E , T_{TOT} , T_I/T_{TOT} , V_T , V_P , $ET-CO_2\%-A$, $t^\circ C Mask$, $U\% Mask$, $P-Mask Pasc$, $t^\circ C timp$ and $PO aur$, HR and sinus arrhythmia kinetics ($HRarrh$). Furthermore, the mean value of the $P-Mask Pasc$ variations caused by the tussian events simulated by the tested subjects was also identified; the dedicated software provided the mean values \pm SD of all the variables for each of the 3 respiratory phases considered and these were compared with appropriate statistical methods in order to detect or not differences.

3 RESULTS AND DISCUSSION

The analysis of instrumental data independently carried out by experts in the analysis of bioelectrical signals, gave a morphological-quantitative evaluation of reliable quality

compared to those expected based on the anthropometric characteristics of the sample of tested subjects.

Tables Ia and Ib show the mean values \pm SD relative to the chosen variables. With regard to HS_{arrh} , the results highlighted that during the Pre-Test the cycle of ortho-parasympathetic activity on heart rate was about 5 heartbeats while in the test phase the neurovegetative regulation mechanism of HS_{arrh} was not efficient. During the Post-Test phase, HS_{arrh} reappeared with an average duration of 5 beats. However, due to this in this case no significant information from the HS_{arrh} data could be acquired. The results of this technological validation of the wearable anti COVID-19 device, carried out in a relevant work environment, reasonably consent us to consider the experiment as successful.

Table Ia

	F_R br/ min	T_I s	T_E s	T_{TOT} s	T_I/T_{TOT}	V_T mL	V_P L/ min
Pre-Test	14.3* ± 3	1.6* ± 0.3	2.6* ± 0.3	4.2* ± 0.3	0.38* ± 0.03	452 ± 48	6.5* ± 1.3
Test	26.1 ± 5	1.2 ± 0.4	1.1 ± 0.5	2.3 ± 0.5	0.69 ± 0.05	431 ± 54	11.3 ± 1.6
Post-test	14.6* ± 6	1.7* ± 0.3	2.4* ± 0.3	4.1* ± 0.5	0.41* ± 0.04	445 ± 51	6.5* ± 1.0
Cough	14.3* ± 3						

Table Ib

	$ET-CO_2$ %	HR Be/ min	P_{Mask} Pasc	t_{Timp} $^\circ C$	U_{Mask} %	P_{Oaur} %
Pre-Test	4.71* ± 0.3	67.2 ± 10.9	101.4 ± 0.6	36.6 ± 0.9	89.8 ± 1.5	98.2 ± 0.2
Test	4.43 ± 0.5	71.1 ± 12.3	101.8 ± 0.9	36.7 ± 1.0	93.3 ± 1.6	98.1 ± 0.4
Post-test	4.68* ± 0.4	66.6 ± 16.1	101.6 ± 0.8	36.8 ± 1.2	91.2 ± 1.7	97.9 ± 0.1
Cough			232.7 ± 13.4			

Tables Ia and Ib show the mean values \pm SD relative to the variables acquired by the tested subjects.

(*) Significant difference ($P < 0.05$) compared to the value detected in the condition (Test), by the statistical test of Student's t for paired data. In fact, from a methodological point of view, the simulation of a non-ergogenic tachypnea was reliable since during the Test phase a R_F was obtained which, on average, was double compared to the Pre and Post-Test conditions. This happened thanks to a significant fall in T_I and T_E and, consequently, in T_{TOT} (- 45%) while the V_T didn't reduced despite the increase in V_P (+ 74%).

Nevertheless, the fact that the inspiratory duty cycle: T_I/T_{TOT} , did not show a reduction during the Test (there was indeed a large and significant increase of 82%) was in line with the occurrence that, being healthy subjects who simulated a non-ergogenic tachypnea, the nervous control system of the respiratory rhythm still maintained its basic setting. However, what was particularly qualifying in this experiment was that, during the test duration interval, the $ET-CO_2\%-A$ was significantly reduced (- 6%) compared to the Pre-Test condition, thus simulating perfectly the case of a hypocapnic tachypnea [26] which could be found as prodromal of a COVID-19 infection. It is also of interest that, during the Test phase, the HS_{arrh} did not manifest as expected, due to the fact that the duration of each breath was too rapid compared to the hemodynamic time constant of this phenomenon which involves the transport of blood from the venous compartment to the arterial compartment of the heart, and this is what we might expect in case of infection with COVID-19. Finally, as can be expected, in a short period of time, the values of t_{Mask} , U_{Mask} and P_{Mask} during the three experimental phases did not show variations as in healthy subjects it is expected for HR , t_{imp} and PO_{aur} . Obviously, these last three variables presented perfectly physiological mean values.

REFERENCES

- [1] Abbas H.S.M., Xu X., Sun C., Ullah A., Gillani S., Raza M.A.A., Impact of COVID-19 pandemic on sustainability determinants: A global trend. *Heliyon*, Vol. 7, No. 2, pp e05912, 2021.
- [2] Rappuoli R., De Gregorio E., Del Giudice G., Phogat S., Pecetta S., Pizza M., Hanon E., Vaccinology in the post-COVID-19 era. *Proc Natl Acad Sci U S A*. Vol. 118, No. 3, pp e2020368118, 2021.
- [3] Kabir H., Maple M., Usher K.J., The impact of COVID-19 on Bangladeshi readymade garment (RMG) workers. *Public Health (Oxf)*. Vol. 43, No.1 pp 47-52, 2021.
- [4] Flocks J, The Potential Impact of COVID-19 on H-2A Agricultural Workers. *J Agromedicine*. Vol. 25, No. 4, pp 367-369, 2020.
- [5] Mix J., Elon L., Vi Thien Mac V., Flocks J., Economos E., Tovar-Aguilar A.J., Stover Hertzberg V., McCauley L.A., Hydration status, kidney function and kidney injury in Florida agricultural workers. *J Occup Environ Med*, Vol. 60, pp e253–e260, 2018.
- [6] Al-Ramahi M., Elnoshokaty A., El-Gayar O., Nasralah T., Wahbeh A., Public Discourse Against Masks in the COVID-19 Era: Infodemiology Study of Twitter Data. *JMIR Public Health Surveill*, Vol. 7, No. 4, e26780, 2021.
- [7] Fadare O.O., Okoffo E.D., Covid-19 face masks: A potential source of microplastic fibers in the environment. *Sci Total Environ*. Vol. 737, pp 140279, 2020.
- [8] Fois A., Tocco F., Dell’Osa A., Melis L., Bertelli U., Concu A., Manuello Bertetto A., Serra C., Innovative smart face mask to protect workers from COVID-19 infection. *Proceedings of the IEEE/MeMeA Symposium on Medical Measurements and Applications*. July 23-25, Neuchatel, Switzerland. (accepted), 2021.
- [9] Chan K.H., Peiris J.S., Lam S.Y., Poon L.L.M., Yuen K.Y., Seto W.H., The effects of temperature and relative humidity on the viability of the SARS coronavirus. *Advances in virology*, Vol. 2011, pp 1-7, 2011.
- [10] Sen A., Khona D., Ghatak S., Gopalakrishnan V., Cornetta K., Ro, S., Khanna S., Sen C., Electroceutical Fabric Lowers Zeta Potential and Eradicates Coronavirus Infectivity upon Contact. Preprint, ChemRxiv. DOI:10.26434/chemrxiv.12307214, 2020.
- [11] Carcassi A.M., Concu A., Decandia M., Onnis M., Orani G.P., Piras M.B., Respiratory Responses to Stimulation of Large Fibers Afferent From Muscle Receptors in Cats. *Pflugers Arch*, Vol. 399, No. 4 pp 309-14. 1983.
- [12] Concu A., Contribution of Central and Reflex Nervous Activity to the Rapid Increase in Pulmonary Ventilation at the Start of Muscular Exercise in Man. *Eur J Appl Physiol Occup Physiol*, Vol. 9, No. 1-2, pp10-15, 1989.
- [13] Swanson P.A., Mc Gavern D.B., Viral Diseases of the Central Nervous System. *Curr Opin Virol*, Vol. 11, pp 44-54 2015.
- [14] Miki K., Tsujino K., Edahiro R., Kitada S., Miki M., Yoshimura K., Kagawa H., Oshitani Y., Ohara Y., Hosono Y., Kurebe H., Maekura R., Exercise tolerance and balance of inspiratory-to expiratory muscle strength in relation to breathing timing in patients with chronic obstructive pulmonary disease. *J Breath Res*, Vol. 12, No. 3, pp 036008, 2018.
- [15] Mo X., Jian W, Su S., Chen M., Peng H., Peng P., Lei C., Chen R., Zhong N., Li S., Abnormal pulmonary function in COVID-19 patients at time of hospital discharge. *Eur Respir J*, Vol. 55, No. 6, pp 2001217, 2020.
- [16] Liu K., Zhang W., Yang Y., Zhang J., Li Y, ChenY., Respiratory rehabilitation in elderly patients with COVID-19: A randomized controlled study. *Complement. Ther Clin Pract* May; Vol. 39, pp 101166, 2020.
- [17] Zheng Y.Y., Ma Y.T., Zhang J.Y., Xie X., COVID-19 and the cardiovascular system. *Nature Reviews Cardiology*, Vol. 17, No. 5, pp 259-260, 2020.
- [18] Kay J.D, Petersen E.S., Vejby-Christensen H., Mean and breath-by-breath pattern of breathing in man during steady-state exercise. *J Physiol*, Vol. 251, No. 3, pp 657–669, 1975.

-
- [19] Brodie D., Slutsky A.S., Acute Respiratory Distress Syndrome: Advances in Diagnosis and Treatment. *JAMA*, Vol. 319, No. 7, pp 698-710, 2018.
- [20] Concu A., Lai A., Marcello C., Cardiovascular responses to slight voluntary hyperpnea at constant tidal volume in humans. *Med Sci Res*, Vol. 19, 1991.
- [21] Boutellier U.R.S., Farhi L.E., Influence of breathing frequency and tidal volume on cardiac output. *Respiration Physiology*, Vol. 66, pp 123-133, 1986.
- [22] Shi H., Han X., Jiang N., Cao Y., Alwalid O., Gu J., Fan Y., Zheng C., Radiological findings from 81 patients with COVID-19 pneumonia in Wuhan, China: a descriptive study. *Lancet Infect Dis*, Vol. 20, 2020.
- [23] Concu A., Cardiovascular adjustments during exercise: Points and counterpoints. In: *New Insight into Cardiovascular Apparatus during Exercise. Physiological and Physio-pathological Aspects*, Eds: Crisafulli A, Concu A., Research Signpost, Transworld Reseach Network, Kerala, India, 2007.
- [24] Marongiu E., Piepoli M., Milia R., Angius L., Pinna M., Bassareo P., Roberto S., Tocco F., Concu A., Crisafulli A., Effects of acute vasodilation on the hemodynamic response to muscle metaboreflex. *Am J Physiol Heart Circ Physiol*, Vol. 305, pp H1387-H1396, 2013.
- [25] Concu A., Rocchitta A., Ciuti C., Marcello C., Autonomic nervous system dependent differences in haemodynamic responses to mental effort of increasing difficulties. *Functional Neurol*, Vol. 9, pp 53-56, 1994.
- [26] Hakumäki M.O., Seventy years of the Bainbridge reflex. *Acta Physiol Scand*, Vol. 130, No. 2, pp177-85. 1987.
- [27] Tian S., Hu N., Lou J., Chen K., Kang X., Xiang Z., Chen H., Wang D, Liu N., Liu D., Chen G., Zhang, Dou Li, Li J., Lian H., Niu S., Luxi Zhang Y., Zhang J., Characteristics of COVID-19 Infection in Beijing. *J Infect*, Vol. 80, Bo. 4, pp 401-406, 2020.
- [28] Sund-Levander M., Forsberg C, Wahren L.K., Normal Oral, Rectal, Tympanic and Axillary Body Temperature in Adult Men and Women: A Systematic Literature Review. *Scand J Caring Sci*, Vol. 16, No. 2, pp 122-128, 2002.
- [29] Crisafulli A., Melis F., Orrù V., Lener R., Lai C., Concu A., Hemodynamic during a postexertional asystolia in a healthy athlete: a case study. *Med Sci Sport & Exer*, Vol. 32, pp 4-9, 1999.